Cyclic AMP regulates formation of mammary epithelial acini in vitro

Pavel I. Nedvetsky[a], Sang-Ho Kwon[a], Jayanta Debnath[b], and Keith E. Mostov[a,c]
[a]Department of Anatomy, [b]Department of Pathology, and [c]Department of Biochemistry and Biophysics, University of California, San Francisco, San Francisco, CA 94143-2140

ABSTRACT **Epithelial cells form tubular and acinar structures notable for a hollow lumen. In three-dimensional culture utilizing MCF10A mammary epithelial cells, acini form due to integrin-dependent polarization and survival of cells contacting extracellular matrix (ECM), and the apoptosis of inner cells of acini lacking contact with the ECM. In this paper, we report that cyclic AMP (cAMP)-dependent protein kinase A (PKA) promotes acinus formation via two mechanisms. First, cAMP accelerates redistribution of α6-integrin to the periphery of the acinus and thus facilitates the polarization of outer acinar cells. Blocking of α6-integrin function by inhibitory antibody prevents cAMP-dependent polarization. Second, cAMP promotes the death of inner cells occupying the lumen. In the absence of cAMP, apoptosis is delayed, resulting in perturbed luminal clearance. cAMP-dependent apoptosis is accompanied by a posttranscriptional PKA-dependent increase in the proapoptotic protein Bcl-2 interacting mediator of cell death. These data demonstrate that cAMP regulates lumen formation in mammary epithelial cells in vitro, both through acceleration of polarization of outer cells and apoptosis of inner cells of the acinus.**

Monitoring Editor
Alpha Yap
University of Queensland

Received: Feb 1, 2012
Revised: May 30, 2012
Accepted: May 30, 2012

INTRODUCTION

Epithelial organ morphogenesis requires the formation of tubular or acinar structures composed of a sheet of epithelial cells surrounding a hollow lumen. While these epithelial structures usually have a simple architecture, a single layer of cells enclosing a luminal space, they are formed by a variety of mechanisms in different organs and species (Hogan and Kolodziej, 2002; Lubarsky and Krasnow, 2003). Three-dimensional culture of MCF10A mammary epithelial cells has contributed significantly to our understanding of such architecture (Debnath *et al.*, 2003; Debnath and Brugge, 2005). When cultured on a reconstituted extracellular matrix (ECM), MCF10A cells form acini via a stereotypical sequence of events (Debnath and Brugge, 2005). Initially, a single cell proliferates to form a solid spheroid with an outer layer of polarized cells contacting the ECM, and an inner core of cells lacking ECM contact. The lack of ECM engagement with integrin receptors, and the consequent down-regulation of epidermal growth factor receptor (EGFR) and extracellular signal–regulated kinase (ERK) signaling (Reginato *et al.*, 2003) predispose the cells to detachment-induced apoptosis, commonly termed *anoikis* (Frisch and Screaton, 2001; Reginato *et al.*, 2003). The resulting imbalance between prosurvival and proapoptotic signals induces proapoptotic BH3-only family proteins Bcl-2 interacting mediator of cell death (BIM) and Bcl-2 modifying factor (Bmf), causing inner cell death and formation of hollow lumen-containing acini (Reginato *et al.*, 2005, 2003; Schmelzle *et al.*, 2007).

The MCF10A system has also been particularly important in studies on several aspects of carcinogenesis, such as lumen filling (Muthuswamy *et al.*, 2001; Debnath *et al.*, 2002; Zhan *et al.*, 2008). Remarkably, in this model, cells are routinely cultured in the presence of cholera toxin, which raises intracellular cyclical AMP (cAMP) concentrations; however, the role of cAMP during acinar morphogenesis remains unclear. In this study, we examined the role of cAMP in MCF10A acini formation. Initially, cAMP accelerated polarization of outer cells in developing acini and

This article was published online ahead of print in MBoC in Press (http://www.molbiolcell.org/cgi/doi/10.1091/mbc.E12-02-0078) on June 6, 2012.

Address correspondence to: Keith E. Mostov (keith.mostov@ucsf.edu).

Abbreviations used: ANOVA, analysis of variance; BIM, Bcl-2 interacting mediator of cell death; Bmf, Bcl-2 modifying factor; Bnz-cAMP, N^6-benzoyl-cAMP; cAMP, cyclic AMP; CPT-2′-*O*-Me-cAMP, 8-(4-chlorophenylthio)-2′-*O*-methyl-cAMP; CPT-cAMP, 8-(4-chlorophenylthio)-cAMP; DAPI, 4′,6-diamidino-2-phenylindole; DMSO, dimethyl sulfoxide; ECM, extracellular matrix; EGFR, epidermal growth factor receptor; ERK, extracellular signal–regulated kinase; EtBr, ethidium bromide; GAPDH, glyceraldehyde 3-phosphate dehydrogenase; HMEC, human mammary epithelial cells; HPV, human papilloma virus; NMuMG, normal murine mammary gland; pERK, phosphorylated ERK; PKA, protein kinase; qPCR, quantitative PCR; RNAi, RNA interference; ROI, region of interest; TUNEL, terminal deoxynucleotidyl transferase dUTP nick end labeling.

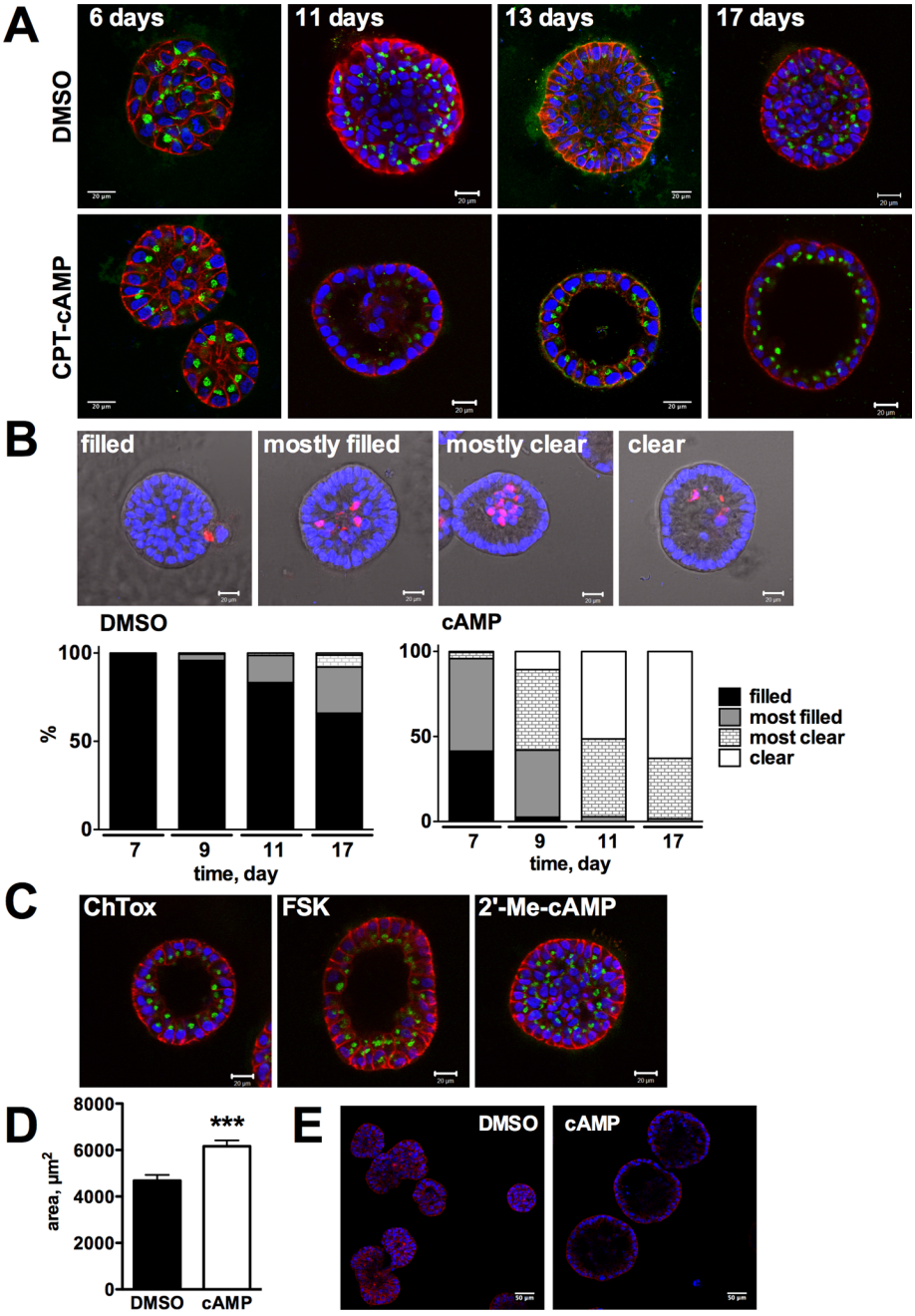

FIGURE 1: cAMP is required for MCF10A acinus formation. (A) MCF10A cells were grown in three-dimensional culture in the absence or the presence of 500 μM CPT-cAMP for different periods of time, and fixed and stained for β-catenin (red), GM130 (green), and nuclei (blue). Scale bars: 20 μm. (B) Top, representative images of acini with filled, mostly filled, mostly clear, and clear lumens. Nuclei were detected by DAPI (blue) and apoptotic cells by cleaved caspase 3 staining (red). Bottom, quantification of acini with varying degrees of luminal filling (as depicted above) when grown in the absence (DMSO, left) or presence of 500 μM CPT-cAMP (right). Data are means of three independent experiments with at least 100 acini counted for each time point. (C) MCF10A cells were grown in three-dimensional culture for 17 d in the presence of 100 ng/ml cholera toxin (ChTx), 10 μM forskolin (FSK), or 500 μM CPT-2′-*O*-Me-cAMP (2′-Me-cAMP), and fixed and stained as in (A). Scale bars: 20 μm. (D) MCF10A cells were grown in the absence (DMSO) and presence (cAMP) of 500 μM CPT-cAMP, and the areas of equatorial cross-sections were measured. Data are mean ± SEM for three independent experiments with more than 100 acini counted for each condition. ***, $p < 0.01$. (E) HPV E7-expressing MCF10A cells were grown in three-dimensional culture for 17 d in the presence or absence of 500 μM CPT-cAMP (cAMP), and fixed and stained to detect nuclei (blue) and F-actin (red). Scale bars: 50 μm.

subsequently lumen clearance by BIM-dependent apoptosis of inner cells.

RESULTS

cAMP is required for MCF10A morphogenesis

Although integrin-dependent and growth factor–dependent signaling are proposed to be the principal regulators of MCF10A acinus formation, we observed that upon removal of cholera toxin, a standard component of the culture medium, MCF10A cells failed to form acini with hollow lumens. Rather, these structures exhibited a significant number of viable cells occupying the luminal space (Figure 1A). At day 17, ~90% of structures growing in the absence of cholera toxin exhibited complete, or near-complete, luminal filling (Figure 1B, right graph). It has been previously demonstrated that the majority of acini have hollow lumens at day 17 if cultured in the presence of cholera toxin (Debnath *et al.*, 2002).

Cholera toxin activates adenylyl cyclase and thus elevates cAMP. To more specifically assess the role of cAMP in acini formation, we tested the effects of a cell-permeable cAMP analogue, 8-(4-chlorophenylthio)-cAMP (CPT-cAMP), on MCF10A morphogenesis. Acini cultured in the presence of CPT-cAMP formed hollow lumens (Figure 1, A and B) with kinetics that closely resembled that of traditional culture in the presence of cholera toxin (Debnath *et al.*, 2002). Similar results were obtained with a second cAMP analogue, dibutyryl-cAMP (unpublished data), and the adenylyl cyclase activator, forskolin (Figure 1C). On the other hand, 8-(4-chlorophenylthio)-2′-*O*-methyl-cAMP (CPT-2′-*O*-Me-cAMP), a cAMP analogue that specifically activates the cAMP-activated guanine nucleotide exchange factor Epac, but not protein kinase A (PKA; Enserink *et al.*, 2002), did not induce lumen formation (Figure 1C; see Supplemental Figure S1A for quantitative results). These data indicate that cholera toxin, forskolin, and cAMP analogues regulate MCF10A morphogenesis in a PKA-dependent and Epac-independent manner.

Increased proliferation does not substitute for cAMP during MCF10A morphogenesis

In MCF10A three-dimensional culture, cell proliferation and formation of solid spherical structures precedes lumen formation. cAMP is known to affect proliferation of mammary epithelial cells (Stampfer, 1982; Ethier *et al.*, 1987; Soule *et al.*, 1990). In MCF10A cells, proliferation can be both

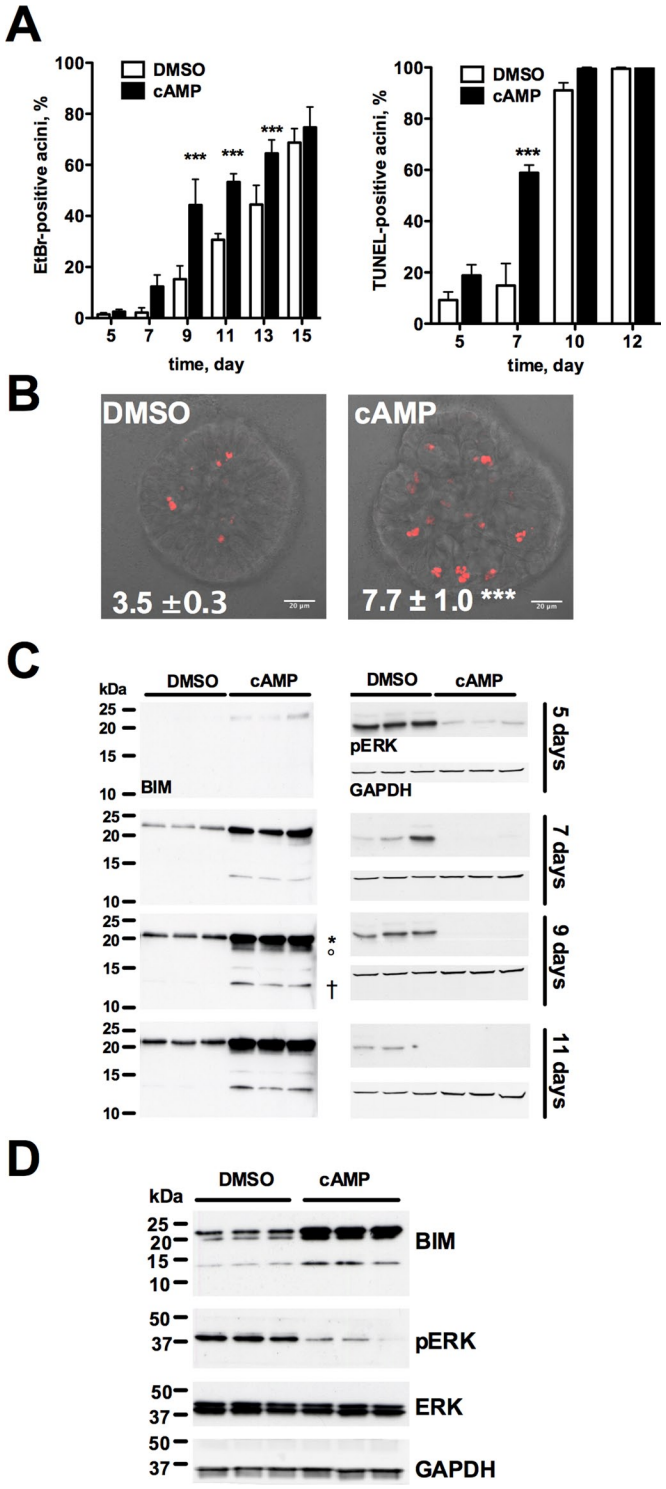

FIGURE 2: cAMP induces luminal apoptosis and increases BIM in MCF10A acini. (A and B) MCF10A cells were grown in three-dimensional culture in the presence or absence of 500 μM CPT-cAMP for indicated times. Dead cells were visualized by EtBr staining (A, left); apoptotic cells were visualized by TUNEL-staining (A, right). Note: positive acini were considered to have at least one EtBr- or TUNEL-positive cell. Quantitative data are means ± SEM of three independent experiments with more than 100 total structures analyzed for each condition. (B) Representative images of 10-d-old TUNEL-stained (red) acini are shown. The numbers on the images are means ± SEM of TUNEL-positive cells per acinus (three independent experiments with 36 and 30 randomly selected acini analyzed for DMSO and cAMP treatment, respectively). Statistically significant differences vs. DMSO-treated cells are indicated: ***, $p < 0.001$. Scale bar: 20 μm. (C) MCF10A cells were grown as in (A). BIM, pERK, and GAPDH were detected by Western blotting. Representative blots are shown. BIM_{EL} (*), BIM_L (°), and BIM_S (†) splice variants are marked. (D) MCF10A cells were grown in three-dimensional culture for 7 d and treated thereafter with 500 μM CPT-cAMP or 0.5% DMSO for another 24 h. BIM, pERK, ERK, and GAPDH were detected by Western blotting.

increased and decreased by cAMP elevation, depending on the cell passage (Soule *et al.*, 1990). Though proliferation was not specifically analyzed, we observed that cAMP-treated acini were slightly, but significantly, larger than control acini at day 17 (Figure 1D). To test whether decreased proliferation may be the reason for affected lumen formation in the absence of cAMP, we examined whether enforced proliferation could substitute for cAMP. For these experiments, MCF10A cells ectopically expressing human papilloma virus (HPV) E7 oncoprotein were used. HPV E7–expressing MCF10A cells proliferated at a much higher rate than control cells (Spancake *et al.*, 1999; Debnath *et al.*, 2002) and failed to undergo proliferative suppression, even after extended periods in three-dimensional culture (Debnath *et al.*, 2002), while control cells became growth-arrested both in the presence and in the absence of cAMP (Figure S1B). Nonetheless, HPV E7-MCF10A acini maintain a hollow polarized structure due to a concomitant increase in luminal apoptosis if cultured in the presence of cholera toxin (Debnath *et al.*, 2002). However, similar to control acini, the formation of a hollow lumen in HPV E7 acini was perturbed in cells cultured in the absence of cholera toxin and restored in the presence of a cAMP analogue (Figure 1E). These results demonstrate that defective MCF10A morphogenesis in the absence of cAMP is not due to affected proliferation, since accelerated proliferation does not substitute for cAMP.

cAMP accelerates luminal apoptosis within MCF10A acini

Lumen formation in MCF10A three-dimensional culture requires death of inner acinar cells. Previous work suggested that the lack of integrin-dependent signaling induces this apoptotic death (Debnath *et al.*, 2002; Reginato *et al.*, 2005). In the presence of cAMP, the fraction of acini containing dead cells in the lumen as monitored by ethidium bromide (EtBr) staining was significantly increased compared with the absence of cAMP elevation (Figure 2A). Next we asked whether this cell death occurs via apoptosis. To assay luminal apoptosis, we performed cleaved caspase 3 and terminal deoxynucleotidyl transferase dUTP nick end labeling (TUNEL) staining. Both the number of cleaved caspase 3- (Figure S1B) and TUNEL-positive acini increased over time (Figure 2A). At earlier time points, the presence of cAMP significantly increased the fraction of cleaved caspase 3– and TUNEL-positive acini. At later time points, when all acini contained apoptotic cells, the number of these cells were higher in the presence than in the absence of cAMP (at day 10, control and cAMP-treated acini contained 3.5 ± 0.3 [$n = 36$] and 7.7 ± 1.0 [$n = 30$] TUNEL-positive cells per acinus, respectively; Figure 2B). This indicates that cAMP accelerates apoptosis of inner cells in MCF10A acini.

cAMP up-regulates the proapoptotic BH3 protein BIM in three-dimensional culture

Both apoptosis and lumen formation in MCF10A acini are regulated by two proapoptotic BH3-only proteins, BIM (Reginato *et al.*, 2005) and Bmf (Schmelzle *et al.*, 2007). These proteins are both induced upon detachment of MCF10A cells from ECM; furthermore, RNA interference (RNAi)-mediated knockdown of either protein results in protection from anoikis and delayed morphogenesis

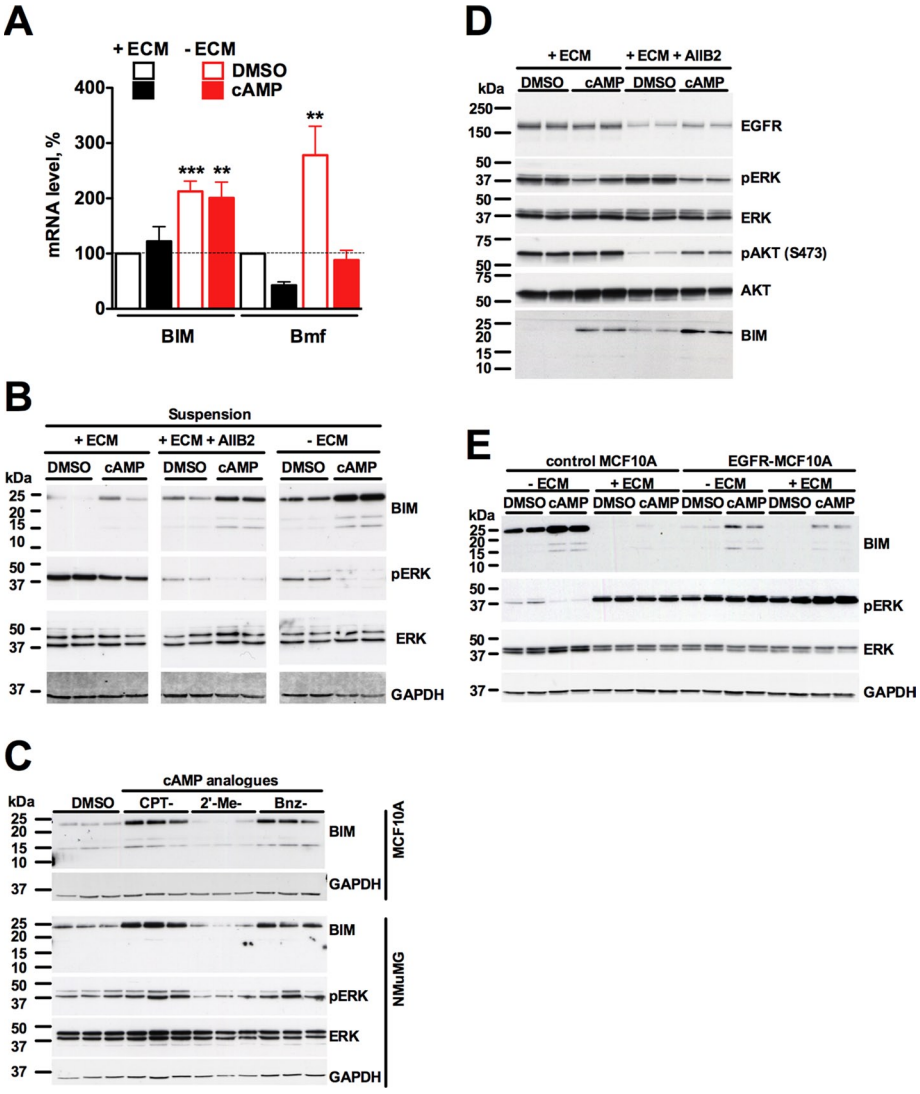

FIGURE 3: cAMP and ECM detachment have distinct and separable effects on BIM and pERK levels in mammary epithelial cells. (A) MCF10A cells were grown in suspension culture in the presence or absence of ECM (2% Matrigel) and/or 500 μM CPT-cAMP. At 24 h, mRNA expression levels of BIM and Bmf were quantified by qPCR and normalized to those for DMSO controls grown in the presence of ECM. Shown are means ± SEM of five independent experiments, each performed in duplicate. Statistically significant differences compared with control (presence of ECM, absence of cAMP; open black bars) are indicated: **, $p < 0.001$; ***, $p < 0.001$. (B) MCF10A cells were grown in suspension culture in the presence or absence of ECM (2% Matrigel) or combination of ECM and inhibiting anti–β1-integrin antibody (AIIB2; 1/200), and treated with 0.5% DMSO or 500 μM CPT-cAMP for 24 h. (C) MCF10A cells or NMuMG cells were treated with 0.5% DMSO, 500 μM CPT-cAMP (CPT-), 500 μM CPT-2′-Me-cAMP (2′-Me-), or 500 μM Bnz-cAMP (Bnz-) for 24 h. (D) Primary HMEC were grown in the presence of ECM (2% Matrigel) or a combination of ECM and inhibiting anti–β1-integrin antibody (AIIB2; 1/200), and treated with 0.5% DMSO or 500 μM CPT-cAMP for 24 h. (E) Control or EGFR-expressing MCF10A cells were grown in suspension culture in the presence or absence of 500 μM CPT-cAMP for 24 h. Indicated proteins were detected by Western blotting.

(Reginato *et al.*, 2005; Schmelzle *et al.*, 2007). Because cAMP regulates intraluminal apoptosis and is required for lumen formation, we studied the effects of cAMP on levels of BIM and Bmf.

We observed that BIM protein levels in MCF10A three-dimensional culture increased over time (Figure 2C), corroborating previous studies (Reginato *et al.*, 2005). At all time points analyzed, the protein levels of BIM, which has three splice isoforms, were significantly higher in the presence than in the absence of cAMP (Figure 2C).

Next we assessed whether cAMP increases BIM protein level by up-regulating BIM mRNA level or by a posttranslational mechanism. Starting at days 7–8, three-dimensional MCF10A cell cultures were treated with CPT-cAMP for 24 h. This acute treatment was sufficient to increase the protein level of BIM (Figure 2D). However, quantitative PCR (qPCR) analysis showed that cAMP did not significantly change BIM mRNA levels under the same conditions (78.7 ± 8.9% of that in dimethyl sulfoxide (DMSO)-treated cells; $p > 0.05$), indicating that the effect of cAMP was posttranscriptional, in contrast to lymphoma cells, in which it has been shown to increase BIM mRNA levels (Zhang and Insel, 2004). While we were unable to detect Bmf at the protein level, cAMP treatment decreased Bmf mRNA levels to 10.1 ± 6.1% of DMSO-treated cells, suggesting that BIM, and not Bmf, mediates cAMP-induced apoptosis in MCF10A acini.

Distinct and separable effects of cAMP and ECM detachment on BIM induction

Because ECM detachment is a strong inducer of BIM (Reginato *et al.*, 2003), we next asked how cAMP impacted these protein levels in ECM-detached cells. MCF10A cells were cultured in suspension with or without cAMP for 24 h; as a control, 2% Matrigel was added to suspension cultures to provide an excess of ECM proteins, ligate integrins and, to some extent, mimic the attachment of the cells to ECM (Reginato *et al.*, 2003). As expected, ECM deprivation resulted in an increase of BIM mRNA (Figure 3A) and protein levels (Figure 3B). In the presence of ECM, addition of β1-integrin–blocking antibody AIIB2 had an effect similar to the absence of ECM (Figure 3B), suggesting an integrin-mediated effect of ECM. Although cAMP did not affect BIM mRNA levels (Figure 3A), it increased the level of BIM protein in the presence or absence of ECM, as well as in the presence of AIIB2 antibody (Figure 3B). Thus ECM detachment and cAMP each have distinct and separable effects on BIM, with ECM detachment increasing BIM expression, and cAMP further increasing BIM protein, but not mRNA levels. As seen in the results obtained in three-dimensional culture, cAMP decreased Bmf mRNA levels both in the presence and in the absence of ECM (Figure 3A), a further indication that Bmf does not have a role in cAMP-dependent apoptosis.

We then studied whether cAMP elevates BIM levels in epithelial cells other than MCF10A. Treatment of suspension cultures of normal murine mammary gland (NMuMG; Figure 3C) cells, primary human mammary epithelial cells (HMEC; Figure 3D), or Madin-Darby canine kidney cells (MDCK; unpublished data) increased BIM

protein levels compared with cells treated with solvent only. These results demonstrate that the cAMP-induced increase in BIM levels is a general phenomenon.

cAMP increases BIM level in a PKA-dependent and ERK-independent manner in mammary epithelial cells

The cAMP-regulated guanine nucleotide exchange factor Epac has been shown to increase transcription of BIM in neuronal cells (Suzuki *et al.*, 2010). Because the Epac-specific activator CPT-2′-*O*-Me-cAMP was not able to induce lumen formation in MCF10A, we hypothesized that cAMP regulates BIM level through a PKA-dependent, Epac-independent mechanism. To test this, we compared the effect of CPT-2′-*O*-Me-cAMP with that of nonselective activator of PKA and Epac, CPT-cAMP, and a PKA-specific activator, N^6-benzoyl-cAMP (Bnz-cAMP). CPT-2′-*O*-Me-cAMP did not increase BIM levels in MCF10A or murine mammary epithelial NMuMG cells cultured in suspension (Figure 3C). In contrast, CPT-cAMP and Bnz-cAMP both increased BIM protein levels in both cell types (Figure 3C).

We have observed that the presence of cAMP in MCF10A three-dimensional culture decreased the level of phosphorylated ERK (pERK; Figure 2, C and D). Because inhibition of ERK signaling results in up-regulation of BIM (Reginato *et al.*, 2003), it is likely that cAMP increases BIM through ERK inhibition. To test whether cAMP can increase BIM in cells preserving a high level of ERK activity, we used EGFR-overexpressing MCF10A cells. These cells have a high level of pERK in suspension and as a result, a low level of BIM (Reginato *et al.*, 2003). Neither the absence of ECM nor the presence of cAMP significantly decreased the pERK levels in these cells in suspension (Figure 3E). However, cAMP still increased BIM in these cells, although to a lower level than in control MCF10A (Figure 3E), suggesting that cAMP can increase BIM even under conditions when ERK activity is preserved.

These data suggest that in mammary epithelial cells cAMP regulates BIM through a PKA-dependent and, at least partially ERK-independent, posttranscriptional mechanism.

cAMP but not detachment induced pERK decrease in primary HMEC

In MCF10A cells cultured in the absence of ECM, EGFR is down-regulated (Reginato *et al.*, 2003). This down-regulation is followed by a strong decrease in the level of pERK (Reginato *et al.*, 2003). Interestingly, pERK showed a greater decrease in the presence than in the absence of cAMP (Figure 3B). These results, together with effects of cAMP on pERK in three-dimensional culture (Figure 2, C and D), suggest that cAMP controls ERK activity in MCF10A cells. To test whether this is true for other mammary epithelial cells, we used primary HMEC. In primary HMEC cultured in the presence of β1-integrin–blocking antibody, the EGFR level went down (Figure 3D). Surprisingly, the down-regulation of EGFR had no effect on ERK phosphorylation. However, pERK was decreased if CPT-cAMP was present (Figure 3D). In contrast to ERK, phosphorylation of AKT was strongly decreased by β1-integrin inhibition, while CPT-cAMP partially restored AKT phosphorylation (Figure 3D). These results suggest that while the EGFR level in mammary epithelial cells is down-regulated by detachment, downstream signaling (ERK and AKT) are differentially modulated by cAMP.

cAMP accelerates polarization of outer acinar cells in an ERK- dependent and α6-integrin–dependent manner

Our data demonstrate that cAMP accelerates lumen formation in MCF10A three-dimensional culture due to increase of BIM protein and intraluminal apoptosis. However, differences between control acini and cAMP-treated acini were obvious before apoptosis started at the stage of polarization. Despite the fact that MCF10A cells do not form tight junctions, outer cells of the acinus acquire several features of polarization during morphogenesis (Debnath and Brugge, 2005). First, these cells became columnar. Second, the Golgi apparatus became oriented to the luminal surface. Third, basement membrane proteins were deposited at the basal surface. We observed that polarization of outer cells was accelerated by the presence of cAMP. At day 6 (3 d after cAMP treatment was started), the majority of CPT-cAMP–treated acini already consisted of a layer of outer cells, which had columnar shape and Golgi apparatus oriented toward the center of the acini, and inner cells of irregular shape. The majority of DMSO-treated acini still consisted of irregularly shaped cells with no clear separation of outer and inner cells (Figures 1A and 4D).

Interaction of integrins with basement membrane proteins is essential for polarization of epithelial cells (Datta *et al.*, 2011). Interestingly, we found that the localization of α6-integrin was affected by cAMP. We measured the percentage of α6-integrin at the peripheral rim around the acinus during the course of polarization (days 4, 5, and 6) in the presence or absence of cAMP. The percentage of α6-integrin at the peripheral rim increased gradually over time and was at every time point higher in the presence than in the absence of cAMP (Figure 4, A and B). We hypothesized that effects of cAMP on α6-integrin localization may be due to inhibition of ERK signaling. To test this, we used the EGFR antagonist, gefitinib, and the MEK inhibitor, U0126. In acini treated with either gefitinib or U0126, outer cells rapidly became columnar (85.5 ± 0.9 and 86.9 ± 5.7 acini were polarized at day 4 in the presence of gefitinib and U0126, respectively), with a peripheral rim of α6-integrin (Figure 4C). Quantification revealed that 51.7 ± 1.0 and 53.2 ± 0.9% of α6-integrin was at the peripheral rim in the presence of gefitinib or U0126, respectively, at day 4. Both of these values were statistically significantly different ($p < 0.001$) compared with DMSO- (34.0 ± 0.7%) or cAMP-treated (44.8 ± 0.8) acini.

Next we explored whether accelerated redistribution of α6-integrin can explain accelerated polarization of outer cells in the presence of cAMP. To test whether inhibition of integrins prevents the polarizing effect of cAMP, we used blocking antibodies against α6-integrin (GoH3) and β1-integrin (AIIB2). Polarization of the outer cells was scored using following parameters: 1) columnar cell shape, 2) orientation of the Golgi apparatus toward the luminal side, and 3) clear separation of outer from inner cells detected by nuclear staining (e.g., see Figure S2). At day 6, 75.2 ± 5.1% and 45.5 ± 7.0% of acini were polarized in the presence and in the absence of cAMP, respectively (Figure 4, D and E). Importantly, while anti–β1-integrin antibody almost completely prevented polarization (5.6 ± 4.3% in polarized acini), anti–α6-integrin antibody decreased cAMP-induced polarization to the level of control acini (44.4 ± 2.1 in polarized acini), suggesting that the cAMP effect was α6-integrin–dependent (Figure 4, D and E).

Next we studied whether inhibition of α6-integrin prevents lumen formation in MCF10A acini. For this purpose, acini were cultured for 17 d in the presence of DMSO, cAMP, or a combination of cAMP and α6-blocking antibody (GoH3). Quantification of the results of these experiments (Figure S1A) demonstrates that GoH3 antibody did not completely prevent, but slowed down, lumen clearance; in the presence of cAMP and GoH3, lumen clearance was intermediate between DMSO- and cAMP-treated cells.

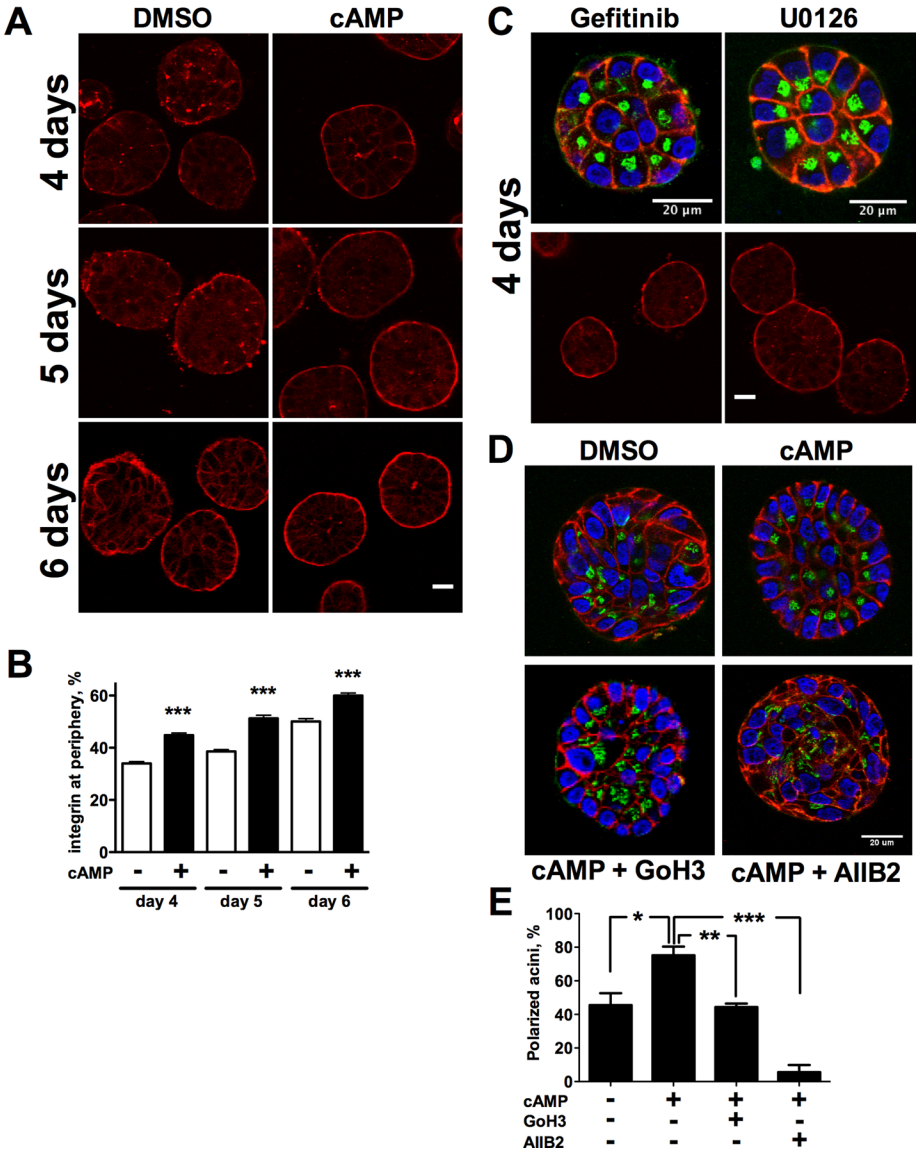

FIGURE 4: cAMP accelerates polarization of MCF10A acini. (A and B) MCF10A acini were treated with 0.5% DMSO or 500 μM CPT-cAMP starting at day 3, fixed at time points indicated, and stained for α6-integrin. Shown are representative images (A) and the percentage of α6-integrin at the peripheral rim of the acinus (B; for quantification details see *Materials and Methods*). Data are means ± SEM of three independent experiments. Between 50 and 90 acini were analyzed for each condition. Statistically significant differences vs. DMSO-treated cells are indicated: ***, $p < 0.001$. (C) MCF10A acini were treated with 10 μM gefitinib or 10 μM U0126 starting at day 3 and were fixed 24 h later. Top, β-catenin (red), GM130 (green), and nuclei (blue); bottom, α6-integrin staining. (D) Day 6 MCF10A acini treated with 0.5% DMSO, 500 μM CPT-cAMP, anti–β1-integrin (AIIB2), or anti–α6-integrin (GoH3 1/50) antibodies and stained for β-catenin (red), GM130 (green), and nuclei (blue). (E) Quantification of percentage of polarized acini at day 6 when treated as indicated in (D). Data are means ± SEM of three independent experiments; more than 100 acini were scored for each condition. Statistically significant differences vs. DMSO-treated cells are indicated: *, $p < 0.05$; **, $p < 0.01$; ***, $p < 0.001$. Scale bars: 20 μm.

β-Adrenergic receptor agonist, isoproterenol, induces lumen formation in MCF10A three-dimensional culture

Elevation of cAMP and activation of PKA mostly follows the activation of Gs protein–coupled receptors. We tested whether activation of such receptors may substitute for the cAMP analogues, cholera toxin and forskolin. We tested the effect of an β-adrenergic agonist, isoproterenol, which elevates cAMP level in acini isolated from lactating rats (Clegg and Mullaney, 1985). Isoproterenol at a concentration of 100 nM induced more than a 20-fold increase in cAMP (Figure 5A). Importantly, similarly to CPT-cAMP, isoproterenol induced formation of hollow polarized acini (Figure 5B).

DISCUSSION

Even in a simplified model of epithelial morphogenesis—in vitro three-dimensional MCF10A cell culture—integration of several signaling pathways is required to form a hollow acinus. Previous studies revealed that integrin-dependent signaling, which allows cells to recognize their position relative to ECM (contacting ECM or trapped within a multicellular structure) is an essential regulator of cell survival or death. In the present study, we describe quite unexpected roles of cAMP and the PKA-dependent pathway in MCF10A morphogenesis.

According to the current model of MCF10A acinus formation, proliferation, polarization, and death of luminal cells are the result of integrin-dependent interaction with ECM. After initial proliferation, the cells that contact ECM become polarized. Integrin-dependent signaling in these cells ensures their survival. In contrast, lack of integrin–ECM interaction in inner cells of the acinus prevents polarization and leads to down-regulation of EGFR with a subsequent decrease in ERK activity (Reginato *et al.*, 2003). This deprives these cells of important survival signals, increases expression of proapoptotic protein BIM, and leads to cell death. However, this view may be not complete. First, we have observed that polarization of MCF10A acini is delayed in conditions in which cAMP is not elevated. cAMP is well known to facilitate polarization of neurons (Shelly *et al.*, 2010; 2011; Cheng *et al.*, 2011). One of the mechanisms is switching ubiquitin E3 ligase Smurf1 substrate preference from Par6 to RhoA due to PKA-dependent phosphorylation (Cheng *et al.*, 2011). Because Smurf1, Par6, and RhoA are also involved in establishing of polarity in epithelial cells (Wang *et al.*, 2003), it remains to be tested whether PKA regulates polarization of epithelial cells via Smurf1 phosphorylation. An alternative mechanism revealed in the present study may be facilitation of integrin redistribution. cAMP facilitates redistribution of α6-integrin to the acinar periphery. The polarizing effect of cAMP could be mimicked by EGFR or ERK inhibition and prevented by inhibitory antibody against α6-integrin. Because cAMP decreases pERK levels in MCF10A three-dimensional culture, we hypothesized that cAMP exerts its polarizing effect through ERK-dependent regulation of α6-integrin.

Importantly, in mammary epithelial cells, detachment from ECM does not inevitably result in down-regulation of ERK signaling. In

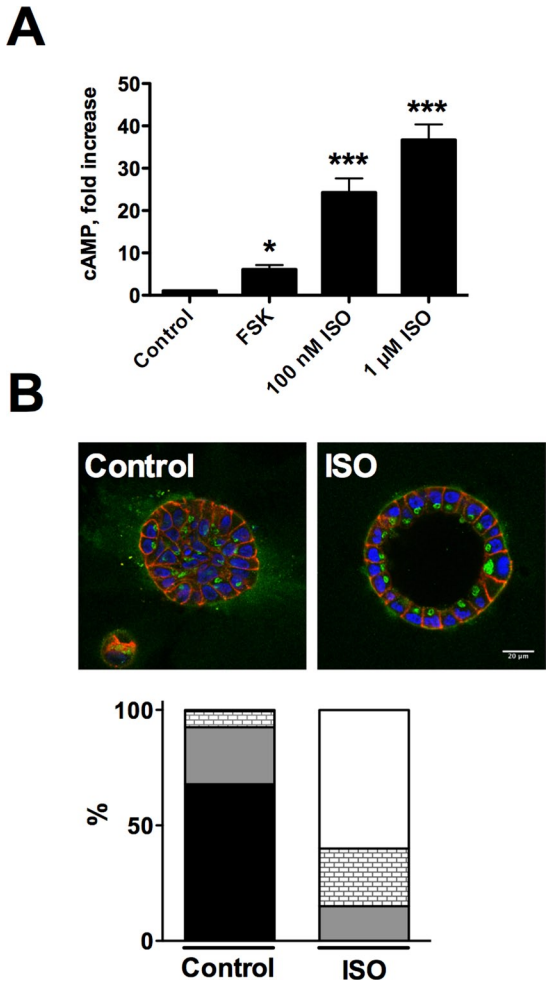

FIGURE 5: β-Adrenergic agonist, isoproterenol, increases cAMP and induces acinus formation in MCF10A cells. (A) MCF10A cells were treated with 10 μM forskolin (FSK) or 100 nM or 1 μM isoproterenol (ISO); cAMP levels were measured and expressed as fold increase of untreated cells. Shown are means ± SEM of three independent experiments. Statistically significant differences vs. control cells are indicated: *, $p < 0.05$; ***, $p < 0.001$. (B) MCF10A cells were grown in three-dimensional culture in the presence or absence of 100 nM isoproterenol (ISO) for 15 d, fixed, and stained for β-catenin (red), GM130 (green), and nuclei (blue). Bottom, quantification of acini with varying degrees of luminal filling (as depicted in Figure 1B) when grown in the absence (Control) or presence (ISO) of 100 nM isoproterenol for 14 d. Data are means of three independent experiments with at least 100 acini counted for each time point.

primary mouse mammary epithelial cells, detachment did not lead to a loss of ERK phosphorylation (Wang *et al.*, 2004). Similarly, in primary cultured HMEC, inhibition of β1-integrin did not affect pERK levels, despite down-regulation of EGFR. On the other hand, cAMP decreased pERK in HMEC. Thus, in MCF10A and other mammary epithelial cells, decreased ERK signaling may result from a combination of integrin- and cAMP-dependent effects, with integrins regulating the levels of EGFR and cAMP acting downstream of the receptor level.

cAMP not only accelerates polarization of outer cells of the acinus, but also increases the rate of luminal apoptosis, which is required to hollow the lumen. Although the decrease in ERK activity may be a reason for the increase of BIM and apoptosis, our data demonstrate that the cAMP effect is at least partially ERK-independent. First, cAMP does not increase BIM mRNA level as detachment and ERK inhibition do (Reginato *et al.*, 2003; Hughes *et al.*, 2011). Second, in MCF10A cells overexpressing EGFR, which have much higher ERK activity and in which cAMP had no effect on ERK activity, cAMP still increased the protein levels of BIM. Third, in NMuMG cells, activation of PKA increased both ERK phosphorylation and BIM protein levels. While this study was in progress, a report describing a posttranslational PKA-dependent stabilization of BIM was published. PKA phosphorylates the largest isoform of BIM, BIM_{EL}, and thus prevents its proteasomal degradation in MCF7 cells (Moujalled *et al.*, 2011). It is likely that the same mechanism is operating in MCF10A cells as well.

Both polarization of the MCF10A acini and intraluminal apoptosis are delayed but not completely prevented in the absence of cAMP. We speculate that the early onset of polarization and apoptosis is important in morphogenesis for elimination of inner cells before they can proliferate, while without this early apoptosis, cells proliferate, more cells occupy the lumen, and the later apoptosis is not able to quickly eliminate them. It is also important to note that lumen formation was not completely prevented but was drastically delayed by the absence of cAMP. It is very likely that MCF10A acini would eventually clear. We were not able to test this hypothesis experimentally, due to matrix destruction and disorganization of three-dimensional structures under prolonged treatment in the absence of cAMP.

Whether cAMP and PKA play a role during normal mammary morphogenesis in vivo in not clear. During puberty, pregnancy, lactation, and involution, mammary glands undergo a complex remodeling that involves multiple hormones and growth factors. At least some of these hormones and growth factors may activate cAMP synthesis (Clegg and Mullaney, 1985; Matsuda *et al.*, 2004; Stull *et al.*, 2007; Pai and Horseman, 2008). We demonstrated here that activation of β-adrenergic receptor is sufficient to mimic effects of cAMP analogues in MCF10A three-dimensional culture.

It is also an interesting question whether deficient cAMP- and PKA-dependent signaling may contribute to epithelial carcinogenesis, since both loss of cell polarity and resistance to apoptosis are hallmarks of carcinogenesis (Debnath and Brugge, 2005).

In summary, in the present study we have demonstrated a novel role for cAMP- and PKA-dependent signaling in regulation of mammary acinus formation. In MCF10A three-dimensional culture, cAMP accelerates polarization of outer acinus cells and apoptosis of inner cells. cAMP exerts its effects both through inhibition of ERK signaling and through ERK-independent elevation of the proapoptotic protein BIM.

MATERIALS AND METHODS

Antibodies and reagents

Commercial antibodies include: rabbit anti-BIM, anti-pERK, anti-ERK, and anti-cleaved caspase 3 (Cell Signaling Technology, Danvers, MA), rabbit anti–β-catenin and rat anti–α6-integrin (GoH3; Santa Cruz Biotechnology, Santa Cruz, CA), mouse anti-GM130 (BD Transduction Laboratories, Lexington, KY), mouse anti–KI-67 (Invitrogen, Carlsbad, CA) and mouse anti–glyceraldehyde 3-phosphate dehydrogenase (GAPDH; Millipore, Billerica, MA). Secondary antibodies include: horseradish peroxidase–coupled (for enhanced chemiluminescence Western blotting) and Alexa Fluor 488 or 555 (for immunostaining), all from Invitrogen. Nuclei were stained with 4′,6-diamidino-2-phenylindole (DAPI; Invitrogen). Growth factor–reduced Matrigel (GFR Matrigel) was from BD Biosciences (San Jose, CA).

Cells

Control MCF10A (either wild-type or retrovirally transduced with pLXSN empty vector), as well as MCF10A cells stably expressing EGFR, have been described elsewhere (Debnath *et al.*, 2002; Reginato *et al.*, 2003). Cells were maintained in DMEM/F12 medium containing 5% horse serum, 20 ng/ml EGF, 10 μg/ml insulin, 0.5 μg/ml cortisol, 100 ng/ml cholera toxin, and 50 U/ml penicillin and 50 mg/ml streptomycin (Debnath *et al.*, 2003). The same medium without cholera toxin was used for suspension assay (see *Suspension Culture*).

Three-dimensional cell culture

Three-dimensional cell culture was performed as previously described (Debnath *et al*. 2003), with minor modifications. Solution of 2% GFR Matrigel was prepared in DMEM/F12 medium containing 2% horse serum, 5 ng/ml EGF, 10 μg/ml insulin, 0.5 μg/ml cortisol, and 50 U/ml penicillin and 50 mg/ml streptomycin. Treatment of cells with cAMP-elevating drugs or inhibitors was started at day 3 after plating the cells onto the three-dimensional culture. Cholera toxin was added to the culture medium only when indicated or, as indicated, replaced by CPT-cAMP, forskolin, or CPT-2′-*O*-Me-cAMP. DMSO was added to cultures as a carrier control when indicated. For immunofluorescence analysis, cells were grown in eight-well chambers (Nunc, Rochester, NY) coated with 10 μl GFR Matrigel; the initial overlay consisted of 5000–6000 cells in 400 μl of media containing 2% GFR Matrigel. For protein biochemistry, cells were grown in 12-well plates coated with 50 μl of GFR Matrigel, with an initial overlay of 50,000 cells in 1 ml of media containing 2% GFR Matrigel. On day 3 following the initial setup, the overlay media was replaced with fresh media containing the indicated cAMP analogues or control media lacking cAMP; thereafter, cultures were fed every 2 d. Luminal filling was examined and scored as described previously (Schafer *et al.*, 2009). Acini were scored as clear (90–100% of luminal space was clear), mostly clear (50–90% clear), mostly filled (10–50% clear), and filled (0–10% clear), as illustrated in Figure 1B.

Suspension culture

For suspension assays, cells were resuspended (250,000 cells/ml) in full medium without cholera toxin, upon which 1 ml of cell suspension was transferred to Ultra-low attachment plates (Corning, Corning, NY). As indicated, CPT-cAMP and/or AIIB2 antibody or GFR Matrigel (at a final concentration of 2%) were added. Cells were incubated for 24 h, harvested, and lysed for Western blotting or RNA isolation.

Immunostaining and microscopy

Immunostaining was performed as described previously (Debnath *et al.*, 2003). Stained acini were analyzed on a LSM 510 laser scanning microscope (Carl Zeiss AG, Jena, Germany) using Plan-Neofluar 25×/0.8 Imm corr DIC objective. Images were captured with Zeiss LSM AIM 4.2 software.

For quantification of EtBr- and TUNEL-positive (Figure 2A) acini, 50–100 acini were scored in each of three independent experiments. Acini were considered to be positive if they contained at least one positive cell.

For quantification of the percentage of α6-integrin at the peripheral rim of the acinus (Figure 4B), fluorescence intensity was measured with ImageJ software. The percentage of α6-integrin at the peripheral rim was calculated as a difference between total α6-integrin intensity (region of interest [ROI] placed right above peripheral rim) and intensity inside the acinus (ROI was placed right below the peripheral rim) after substraction of background.

Western blotting

For preparation of lysates for Western blotting, incubation medium was removed and acini were washed briefly with ice-cold phosphate-buffered saline, directly lysed in SDS sample buffer, and boiled for 5 min. Proteins were separated by SDS–PAGE using a Criterion electrophoresis system (Bio-Rad Laboratories, Hercules, CA), transferred onto the polyvinylidene fluoride membrane, and immunoblotted with specific antibodies.

qPCR

RNA was isolated using the RNEasy Mini kit (Qiagen, Valencia, CA) according to the manufacturer's protocol. RNA (0.8–1.0 μg) was subjected to reverse transcription with Phusion RT-PCR kit (New England Biolabs, Ipswich, MA). qPCR was performed using the DyNAmo Flash SYBR Green qPCR kit (New England Biolabs) on a Stratagene Mx4000 QPCR machine. Changes in mRNA level were calculated according to Δ–ΔC_t method, using GAPDH as a reference.

Measurement of cAMP level

cAMP levels were measured using a commercial enzyme-linked immunoassay kit (#4339; Cell Signaling) according to the manufacturer's instructions.

Statistical analysis

Statistical analysis was performed with GraphPad Prism 5 software (La{thin space}Jolla, CA). For Figures 2, A and B, and 4B, data were analyzed using a two-way analysis of variance (ANOVA) test and statistically significant differences between control (DMSO-treated) and CPT-cAMP–treated acini were calculated using a Bonferroni posttest. For data on Figures 4D and 5A, one-way ANOVA analysis was performed, and statistically significant differences were calculated using a Bonferroni posttest.

ACKNOWLEDGMENTS

This study was supported by National Institutes of Health grants to K.E.M (R01-DK074398 and P01-AI53194), S.-H.K. (DK082115), and J.D (R01-CA126792). P.I.N. was supported by a fellowship from the German Research Society (Ne-897/1-1). We thank David Bryant for his comments on the manuscript.

REFERENCES

Cheng P-L, Lu H, Shelly M, Gao H, Poo M-M (2011). Phosphorylation of E3 ligase Smurf1 switches its substrate preference in support of axon development. Neuron 69, 231–243.

Clegg RA, Mullaney I (1985). Acute change in the cyclic AMP content of rat mammary acini in vitro. Influence of physiological and pharmacological agents. Biochem J 230, 239.

Datta A, Bryant DM, Mostov KE (2011). Molecular regulation of lumen morphogenesis. Curr Biol 21, R126–R136.

Debnath J, Brugge JS (2005). Modelling glandular epithelial cancers in three-dimensional cultures. Nat Rev Cancer 5, 675–688.

Debnath J, Mills KR, Collins NL, Reginato MJ, Muthuswamy SK, Brugge JS (2002). The role of apoptosis in creating and maintaining luminal space within normal and oncogene-expressing mammary acini. Cell 111, 29–40.

Debnath J, Muthuswamy SK, Brugge JS (2003). Morphogenesis and oncogenesis of MCF-10A mammary epithelial acini grown in three-dimensional basement membrane cultures. Methods 30, 256–268.

Enserink JM, Christensen AE, de Rooij J, van Triest M, Schwede F, Genieser HG, Døskeland SO, Blank JL, Bos JL (2002). A novel Epac-specific cAMP analogue demonstrates independent regulation of Rap1 and ERK. Nat Cell Biol 4, 901–906.

Ethier SP, Kudla A, Cundiff KC (1987). Influence of hormone and growth factor interactions on the proliferative potential of normal rat mammary epithelial cells in vitro. J Cell Physiol 132, 161–167.

Frisch SM, Screaton RA (2001). Anoikis mechanisms. Curr Opin Cell Biol 13, 555–562.
Hogan BLM, Kolodziej PA (2002). Organogenesis, molecular mechanisms of tubulogenesis. Nat Rev Genet 3, 513–523.
Hughes R, Gilley J, Kristiansen M, Ham J (2011). The MEK-ERK pathway negatively regulates *bim* expression through the 3′ UTR in sympathetic neurons. BMC Neurosci 12, 69.
Lubarsky B, Krasnow MA (2003). Tube morphogenesis. Cell 112, 19–28.
Matsuda M *et al*. (2004). Serotonin regulates mammary gland development via an autocrine-paracrine loop. Dev Cell 6, 193–203.
Moujalled D, Weston R, Anderton H, Ninnis R, Goel P, Coley A, Huang DCS, Wu L, Strasser A, Puthalakath H (2011). Cyclic-AMP-dependent protein kinase A regulates apoptosis by stabilizing the BH3-only protein Bim. EMBO Rep 12, 77–83.
Muthuswamy SK, Li D, Lelievre S, Bissell MJ, Brugge JS (2001). ErbB2, but not ErbB1, reinitiates proliferation and induces luminal repopulation in epithelial acini. Nat Cell Biol 3, 785–792.
Pai VP, Horseman ND (2008). Biphasic regulation of mammary epithelial resistance by serotonin through activation of multiple pathways. J Biol Chem 283, 30901–30910.
Reginato MJ, Mills KR, Becker EBE, Lynch DK, Bonni A, Muthuswamy SK, Brugge JS (2005). Bim regulation of lumen formation in cultured mammary epithelial acini is targeted by oncogenes. Mol Cell Biol 25, 4591–4601.
Reginato MJ, Mills KR, Paulus JK, Lynch DK, Sgroi DC, Debnath J, Muthuswamy SK, Brugge JS (2003). Integrins and EGFR coordinately regulate the pro-apoptotic protein Bim to prevent anoikis. Nat Cell Biol 5, 733–740.
Schafer ZT, Grassian AR, Song L, Jiang Z, Gerhart-Hines Z, Irie HY, Gao S, Puigserver P, Brugge JS (2009). Antioxidant and oncogene rescue of metabolic defects caused by loss of matrix attachment. Nature 461, 109–113.
Schmelzle T, Mailleux AA, Overholtzer M, Carroll JS, Solimini NL, Lightcap ES, Veiby OP, Brugge JS (2007). Functional role and oncogene-regulated expression of the BH3-only factor Bmf in mammary epithelial anoikis and morphogenesis. Proc Natl Acad Sci USA 104, 3787–3792.
Shelly M, Cancedda L, Lim BK, Popescu AT, Cheng P-L, Gao H, Poo M-M (2011). Semaphorin3A regulates neuronal polarization by suppressing axon formation and promoting dendrite growth. Neuron 71, 433–446.
Shelly M, Lim BK, Cancedda L, Heilshorn SC, Gao H, Poo M-M (2010). Local and long-range reciprocal regulation of cAMP and cGMP in axon/dendrite formation. Science 327, 547–552.
Soule HD, Maloney TM, Wolman SR, Peterson WD, Brenz R, McGrath CM, Russo J, Pauley RJ, Jones RF, Brooks SC (1990). Isolation and characterization of a spontaneously immortalized human breast epithelial cell line, MCF-10. Cancer Res 50, 6075–6086.
Spancake KM, Anderson CB, Weaver VM, Matsunami N, Bissell MJ, White RL (1999). E7-transduced human breast epithelial cells show partial differentiation in three-dimensional culture. Cancer Res 59, 6042–6045.
Stampfer MR (1982). Cholera toxin stimulation of human mammary epithelial cells in culture. In Vitro 18, 531–537.
Stull MA, Pai V, Vomachka AJ, Marshall AM, Jacob GA, Horseman ND (2007). Mammary gland homeostasis employs serotonergic regulation of epithelial tight junctions. Proc Natl Acad Sci USA 104, 16708–16713.
Suzuki S, Yokoyama U, Abe T, Kiyonari H, Yamashita N, Kato Y, Kurotani R, Sato M, Okumura S, Ishikawa Y (2010). Differential roles of Epac in regulating cell death in neuronal and myocardial cells. J Biol Chem 285, 24248–24259.
Wang H-R, Zhang Y, Ozdamar B, Ogunjimi AA, Alexandrova E, Thomsen GH, Wrana JL (2003). Regulation of cell polarity and protrusion formation by targeting RhoA for degradation. Science 302, 1775–1779.
Wang P, Gilmore AP, Streuli CH (2004). Bim is an apoptosis sensor that responds to loss of survival signals delivered by epidermal growth factor but not those provided by integrins. J Biol Chem 279, 41280–41285.
Zhang L, Insel PA (2004). The pro-apoptotic protein Bim is a convergence point for cAMP/protein kinase A- and glucocorticoid-promoted apoptosis of lymphoid cells. J Biol Chem 279, 20858–20865.
Zhan L, Rosenberg A, Bergami KC, Yu M, Xuan Z, Jaffe AB, Allred C, Muthuswamy SK (2008). Deregulation of Scribble promotes mammary tumorigenesis and reveals a role for cell polarity in carcinoma. Cell 135, 865–878.